

Supporting Information

**Syntheses of mono- and diacylated bipyrrroles with rich  
substitution modes and development of a prodigiosin  
derivative as a fluorescent Zn(II) probe**

Tao Hong,<sup>a</sup> Heli Song,<sup>a</sup> Xin Li,<sup>b</sup> Weibing Zhang,<sup>a</sup> and Yongshu Xie<sup>\*a</sup>

<sup>a</sup>Key Laboratory for Advanced Materials and Institute of Fine Chemicals, Shanghai Key  
Laboratory of Functional Materials Chemistry, East China University of Science and Technology,  
Shanghai 200237, P. R. China. <sup>b</sup>Department of Theoretical Chemistry and Biology, School of  
Biotechnology, KTH Royal Institute of Technology, Stockholm, Sweden

E-mail: yshxie@ecust.edu.cn

Contents

Characterization data for compounds 1 ~ 6 and 8~9.....	Pages S2~S11
Job's plot, Determination of $K_{ass}$ for 9 with $Zn^{2+}$ .....	Pages S12
Detection limit of 9.....	Page
S	1 3
Titration of 9 with $Zn^{2+}$ in HEPES buffer.....	Page S13

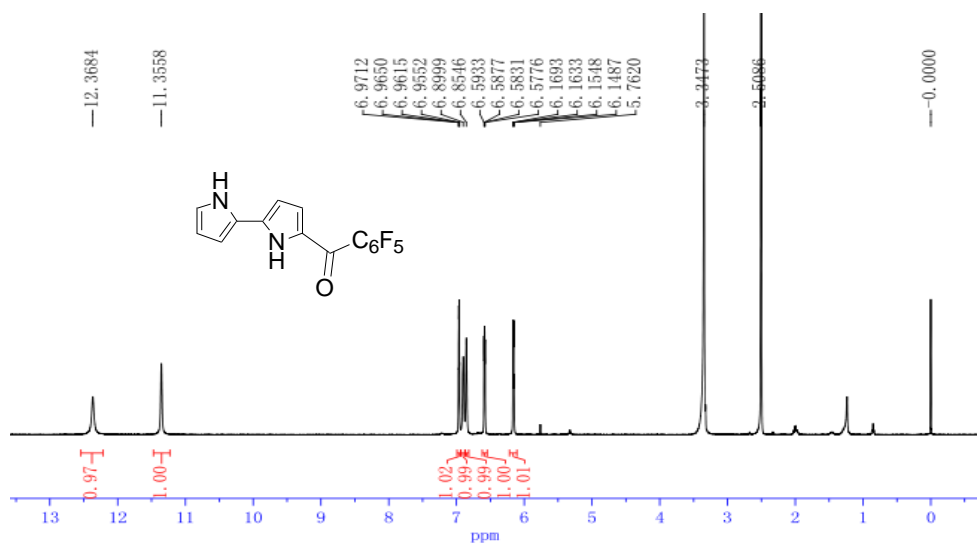


Figure. S1. The  $^1\text{H}$  NMR spectrum of **1** in  $\text{DMSO-}d_6$ .

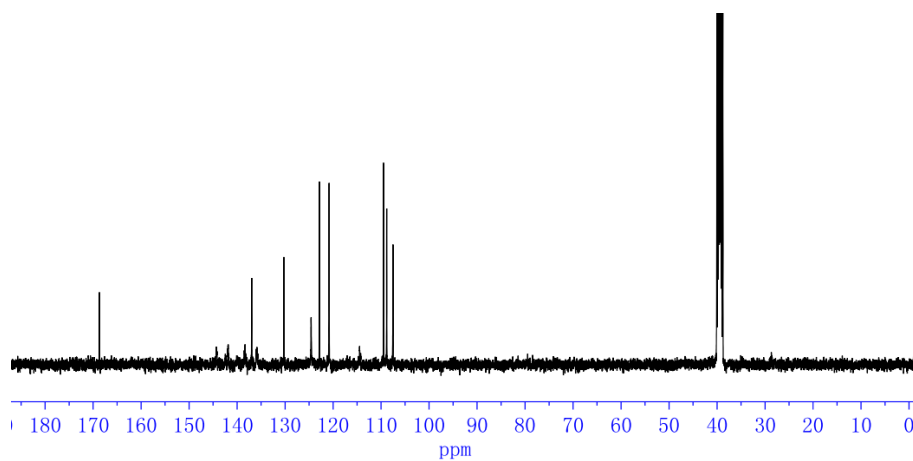


Figure. S2. The  $^{13}\text{C}$  NMR spectrum of **1** in  $\text{DMSO-}d_6$ .

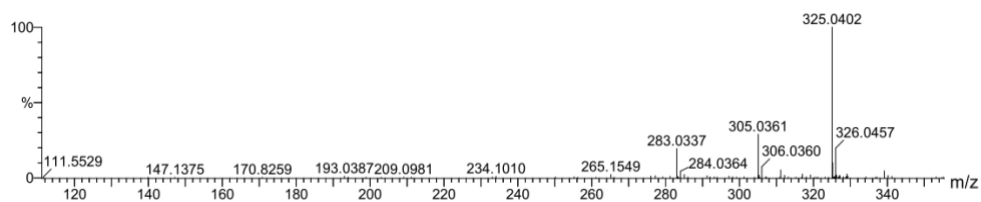


Figure. S3. ESI-HRMS of **1** in MeOH.

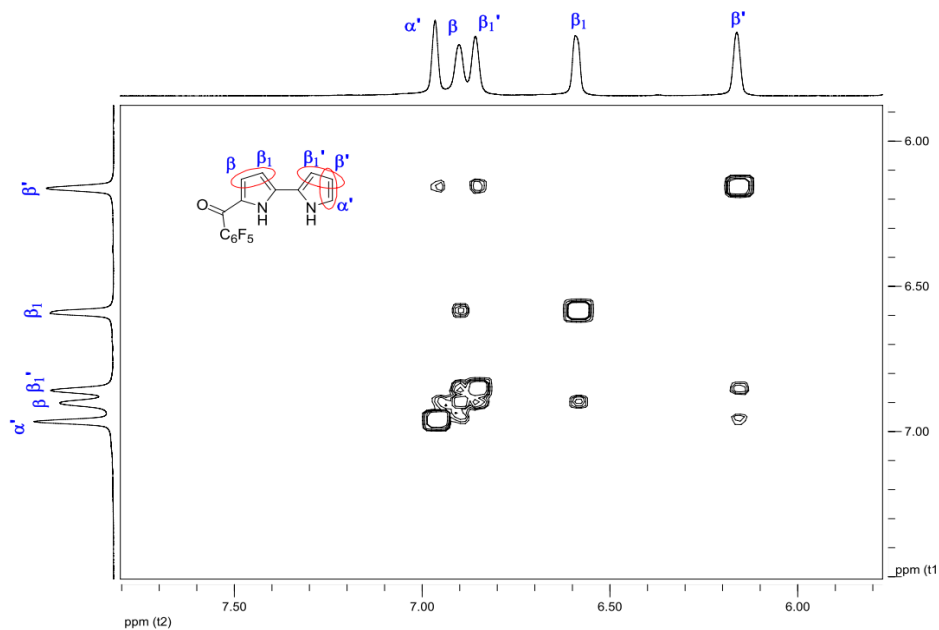


Figure S4. The  $^1\text{H}$ - $^1\text{H}$  COSY NMR spectrum of **1** (500 MHz in  $\text{DMSO-}d_6$  at 298K).

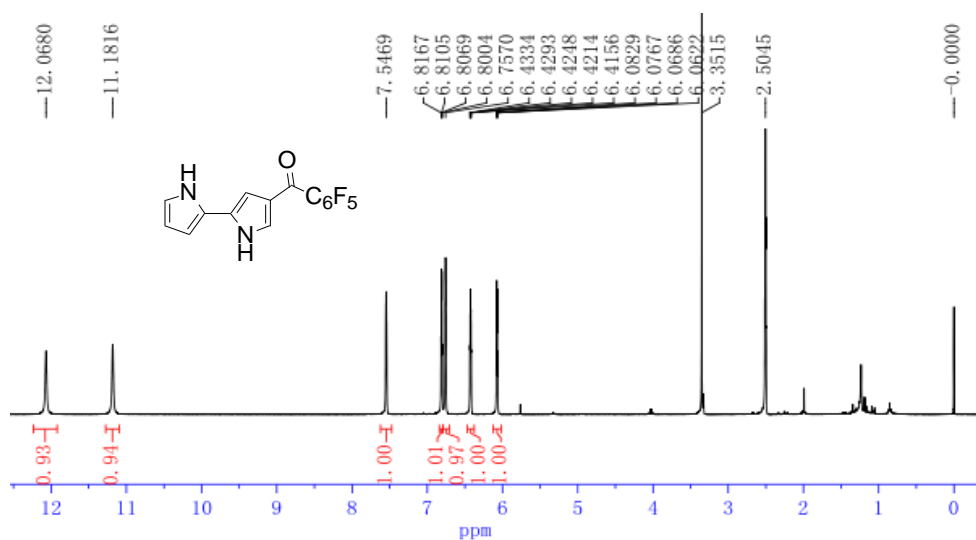


Figure. S5. The  $^1\text{H}$  NMR spectrum of **2** in  $\text{DMSO-}d_6$ .

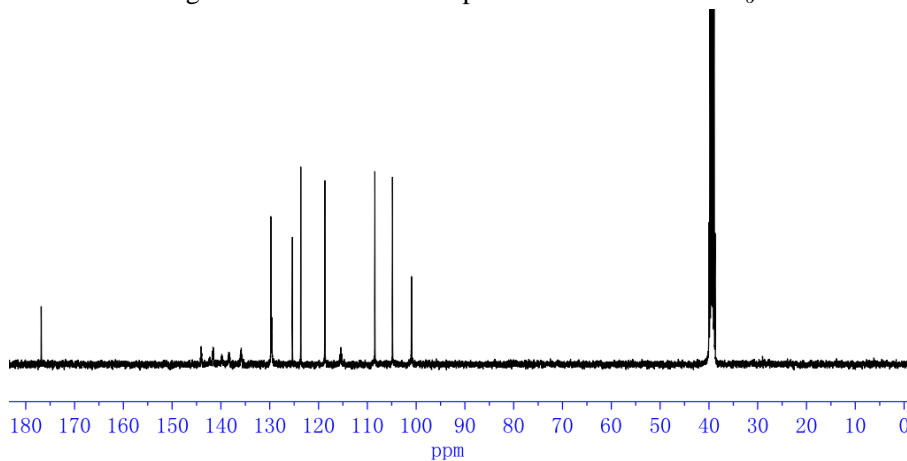


Figure. S6. The  $^{13}\text{C}$  NMR spectrum of **2** in  $\text{DMSO-}d_6$ .

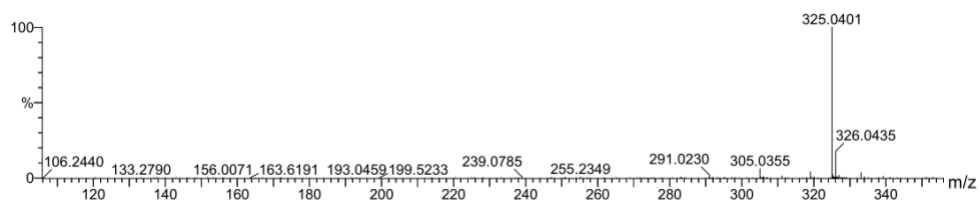


Figure. S7. ESI-HRMS of **2** in MeOH.

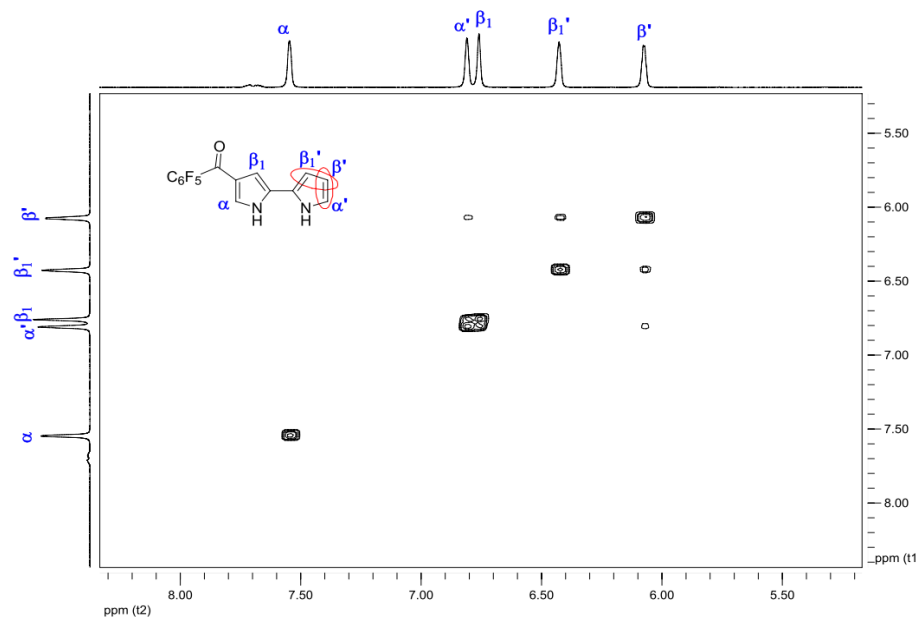


Figure. S8. The  $^1\text{H}$ - $^1\text{H}$  COSY NMR spectrum of **2** (500 MHz in  $\text{DMSO-}d_6$  at 298K).

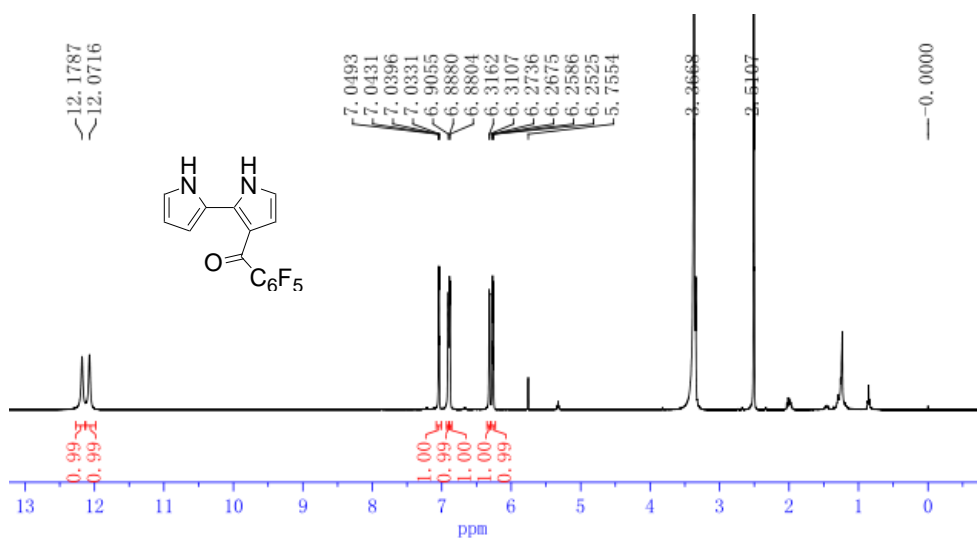


Figure. S9. The  $^1\text{H}$  NMR spectrum of **3** in  $\text{DMSO-}d_6$ .

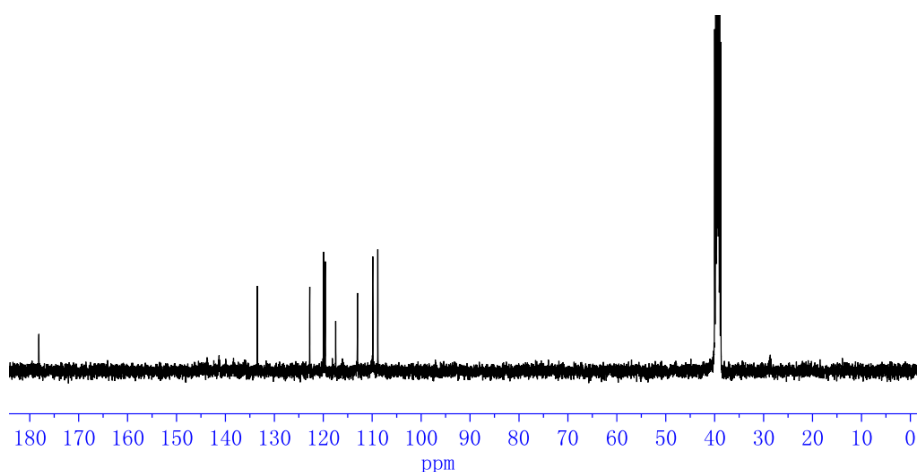


Figure. S10. The  $^{13}\text{C}$  NMR spectrum of **3** in  $\text{DMSO-}d_6$ .

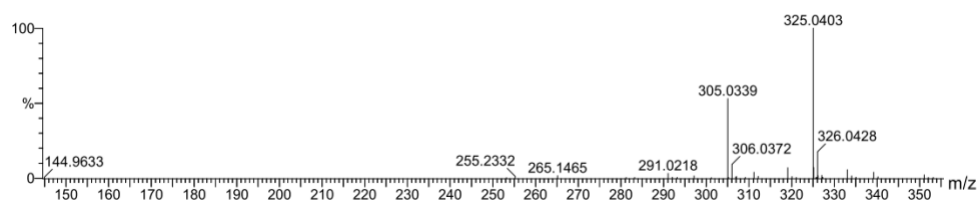


Figure. S11. ESI-HRMS of **3** in MeOH.

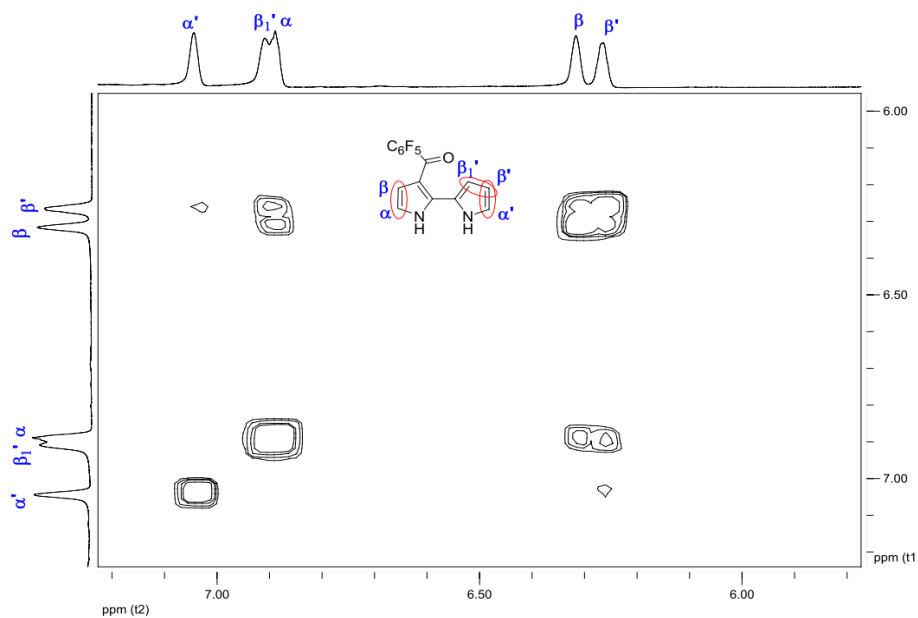


Figure. S12. The  $^1\text{H-}^1\text{H}$  COSY NMR spectrum of **3** (500 MHz in  $\text{DMSO-}d_6$  at 298K).

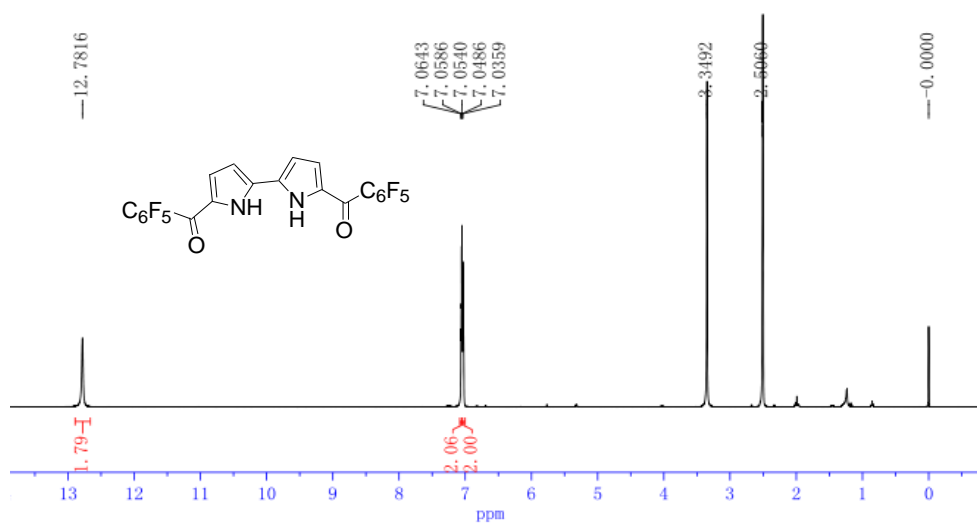


Figure. S13. The  $^1\text{H}$  NMR spectrum of **4** in  $\text{DMSO-}d_6$ .

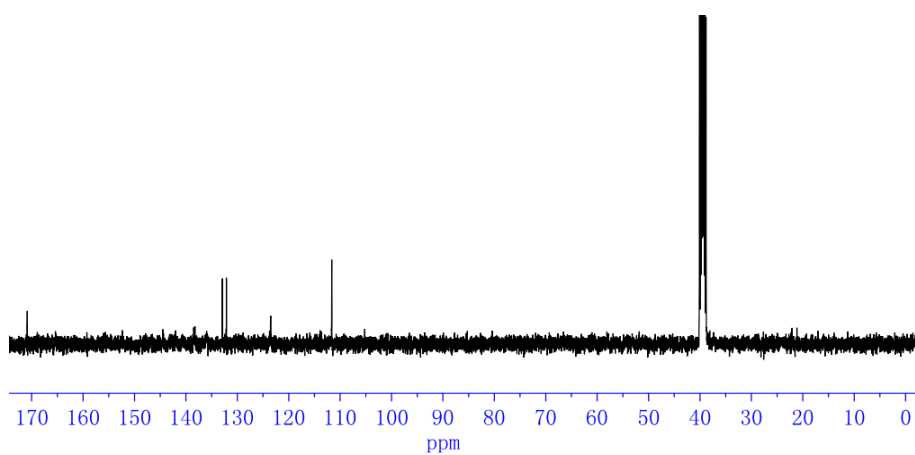


Figure. S14. The  $^{13}\text{C}$  NMR spectrum of **4** in  $\text{DMSO-}d_6$ .

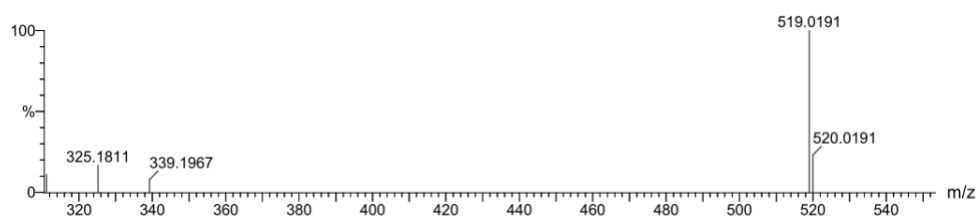


Figure. S15. ESI-HRMS of **4** in MeOH.

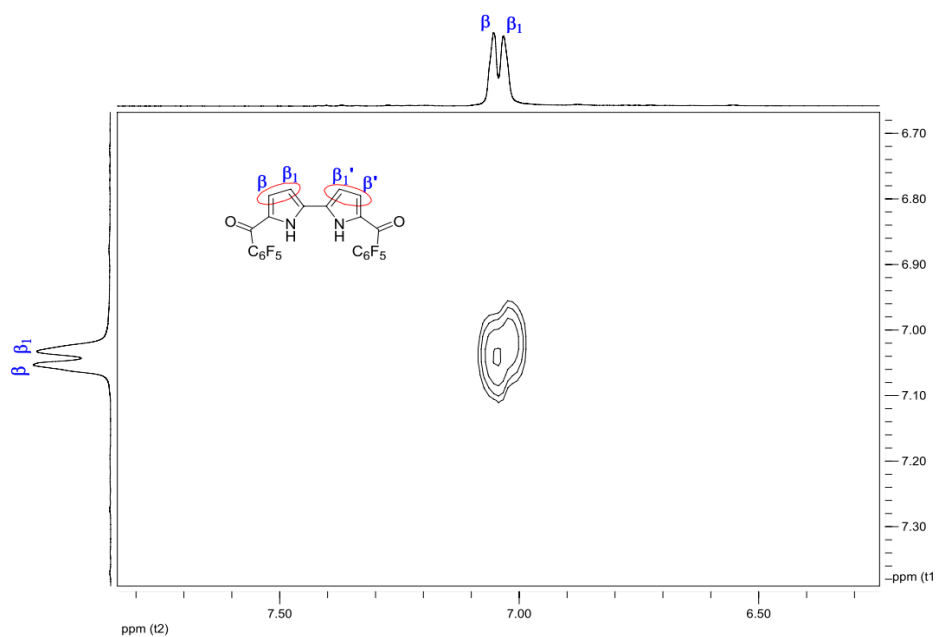


Figure. S16. The  $^1\text{H}$ - $^1\text{H}$  COSY NMR spectrum of **4** (500 MHz in  $\text{DMSO-}d_6$  at 298K).

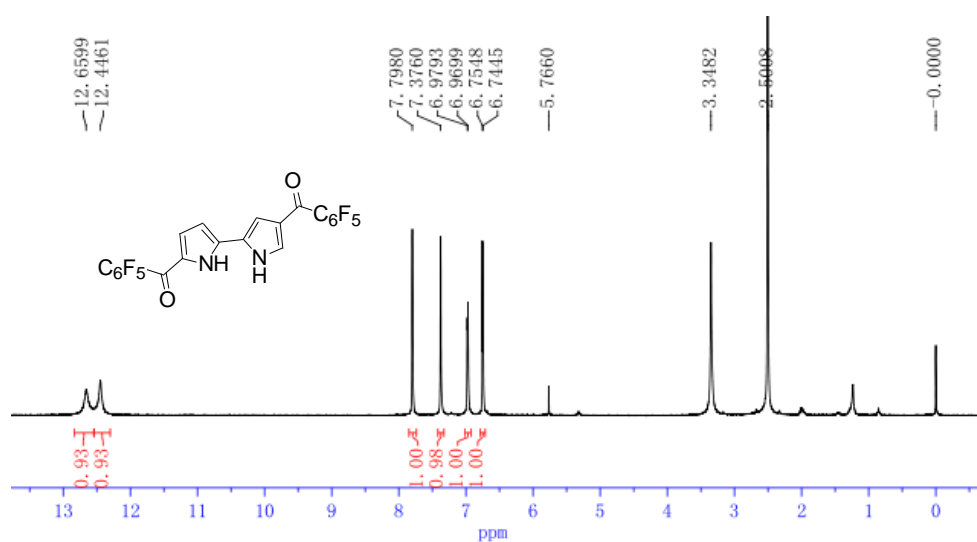


Figure. S17. The  $^1\text{H}$  NMR spectrum of **5** in  $\text{DMSO-}d_6$ .

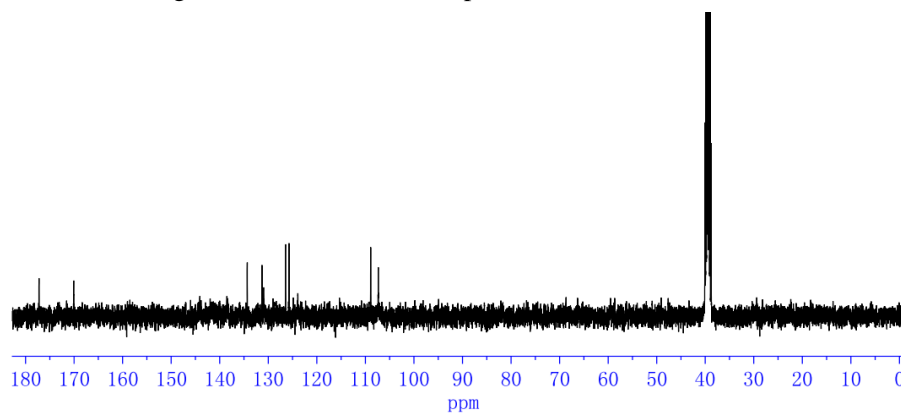


Figure. S18. The  $^{13}\text{C}$  NMR spectrum of **5** in  $\text{DMSO-}d_6$ .

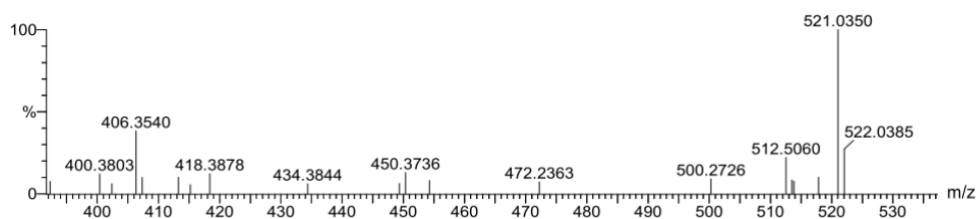


Figure. S19. ESI-HRMS of **5** in MeOH.

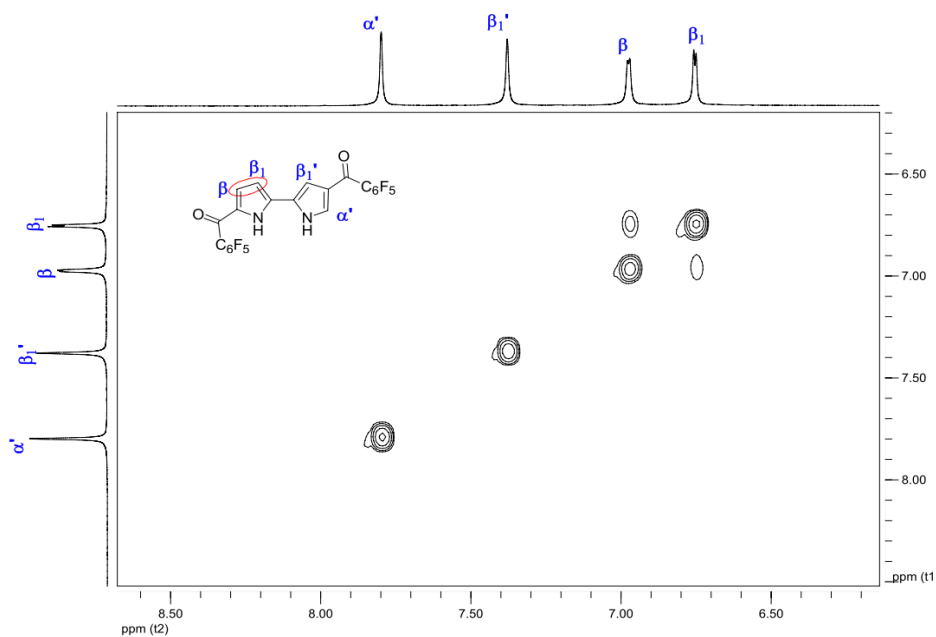


Figure. S20. The  $^1\text{H}$ - $^1\text{H}$  COSY NMR spectrum of **5** (500 MHz in  $\text{DMSO-}d_6$  at 298K).

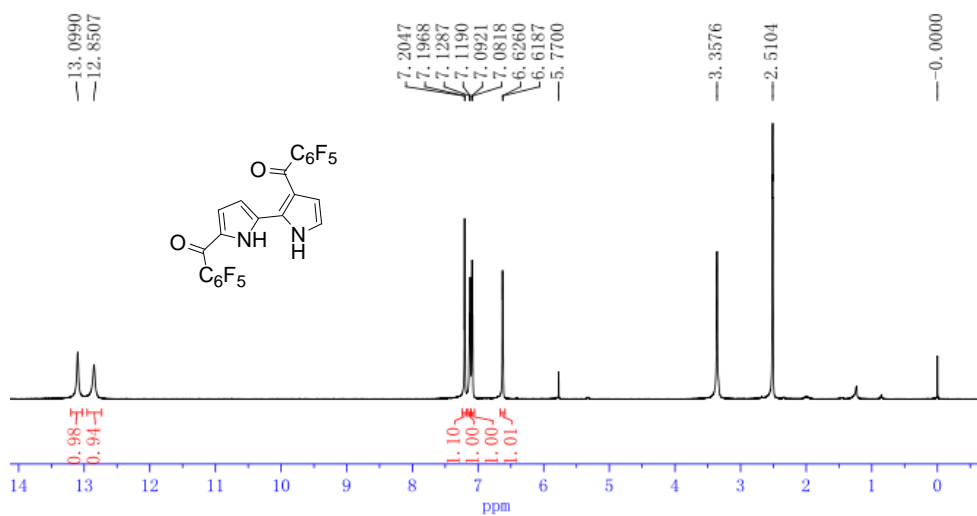


Figure. S21. The  $^1\text{H}$  NMR spectrum of **6** in  $\text{DMSO-}d_6$ .



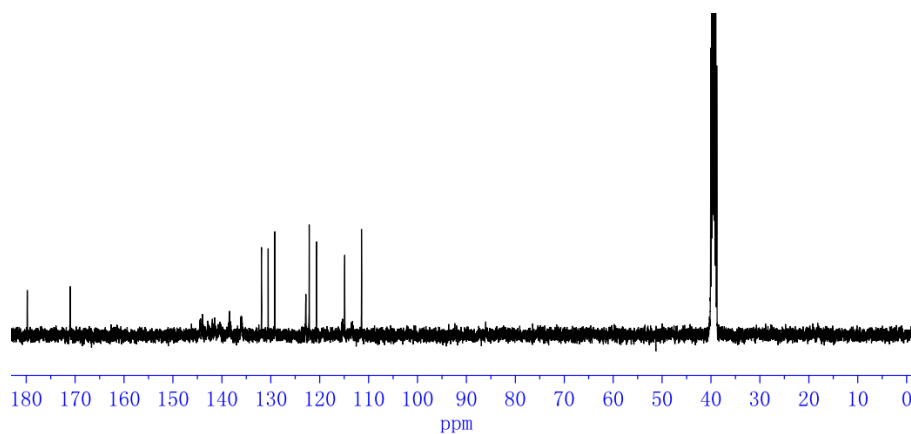


Figure. S22. The  $^{13}\text{C}$  NMR spectrum of **6** in  $\text{DMSO-}d_6$ .

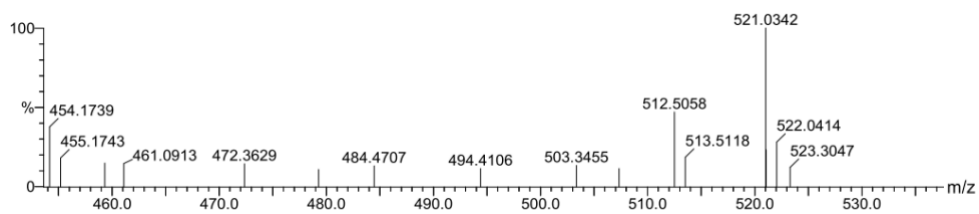


Figure. S23. ESI-HRMS of **6** in MeOH.

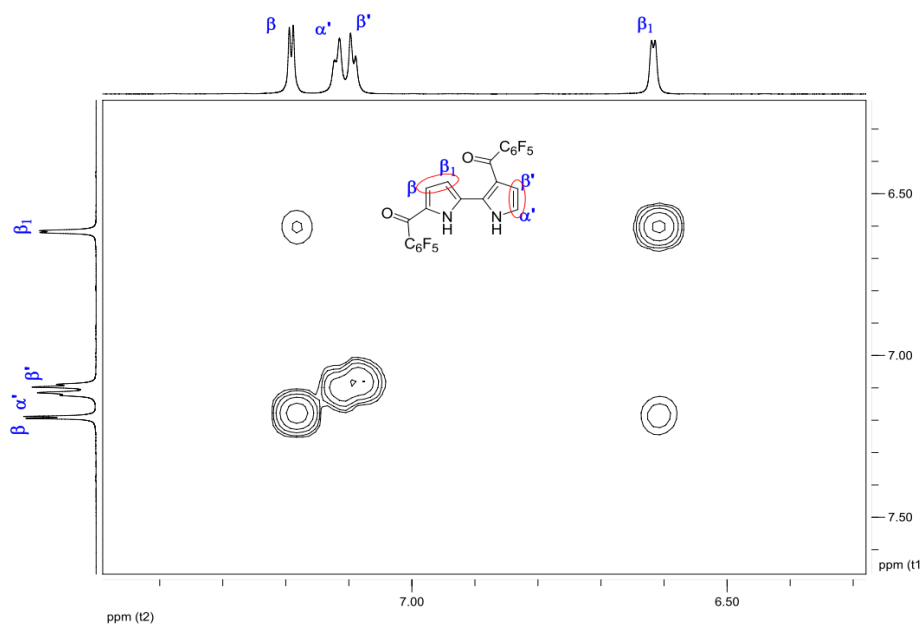


Figure. S24. The  $^1\text{H-}^1\text{H}$  COSY NMR spectrum of **6** (500 MHz in  $\text{DMSO-}d_6$  at 298K).

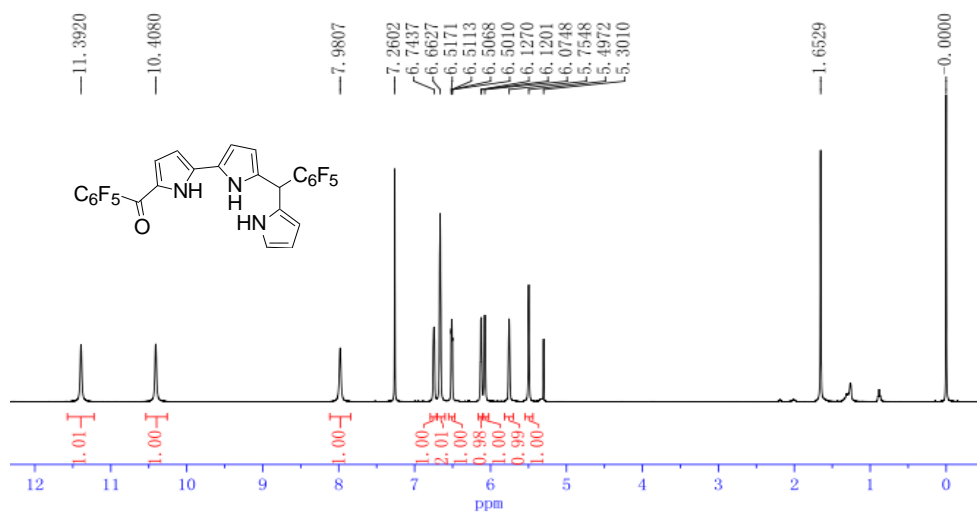


Figure. S25. The <sup>1</sup>H NMR spectrum of **8** in CDCl<sub>3</sub>.

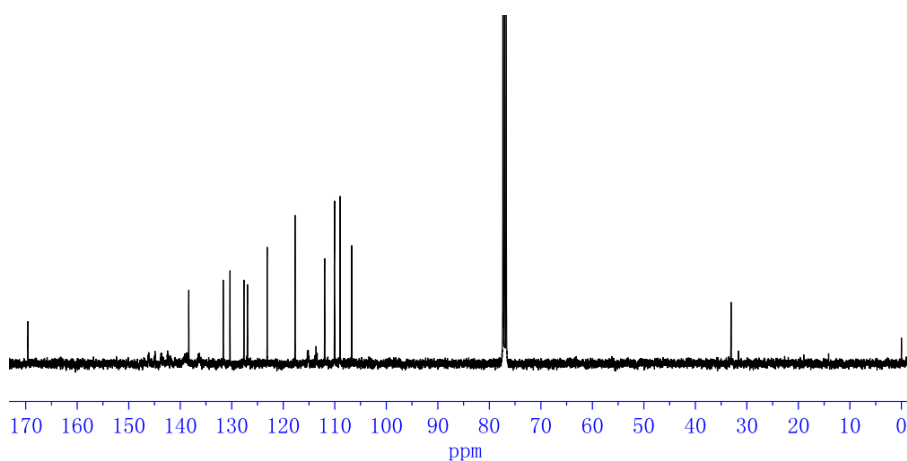


Figure. S26. The <sup>13</sup>C NMR spectrum of **8** in CDCl<sub>3</sub>.

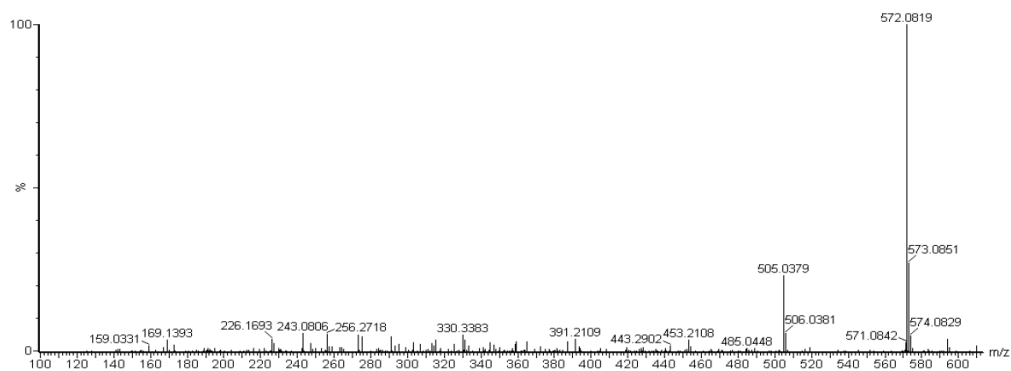


Figure. S27. ESI-HRMS of **8** in MeOH.

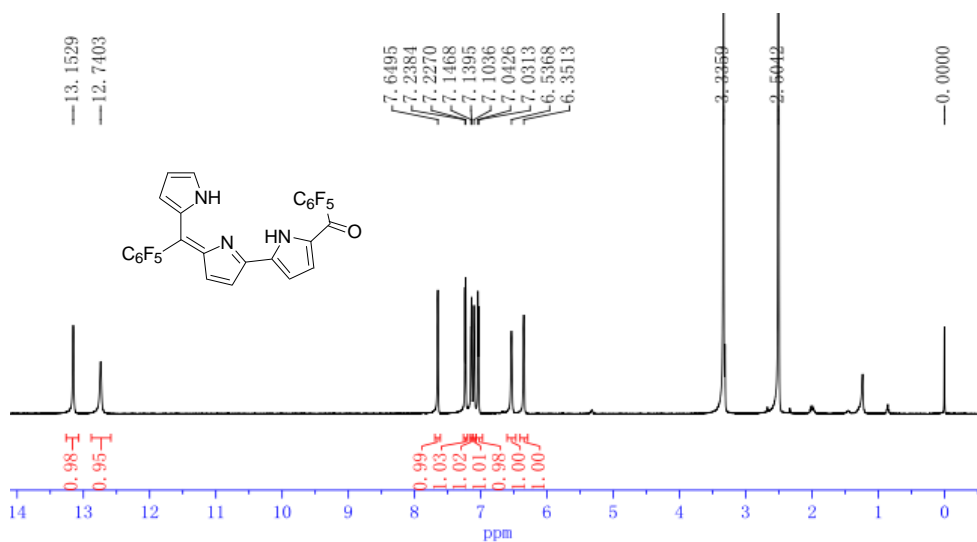


Figure. S28. The  $^1\text{H}$  NMR spectrum of **9** in  $\text{DMSO-}d_6$ .

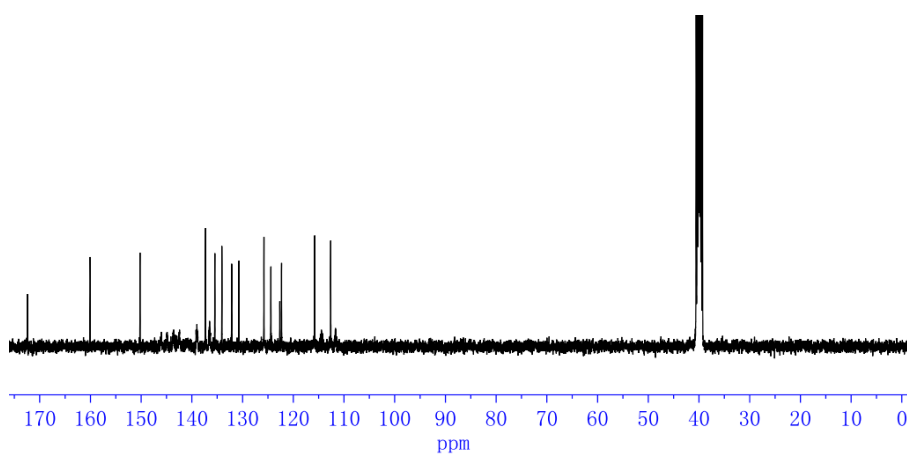


Figure. S29. The  $^{13}\text{C}$  NMR spectrum of **9** in  $\text{DMSO-}d_6$ .

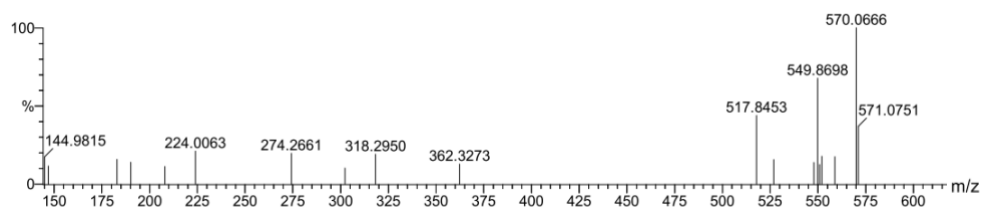


Figure. S30. ESI-HRMS of **9** in MeOH.

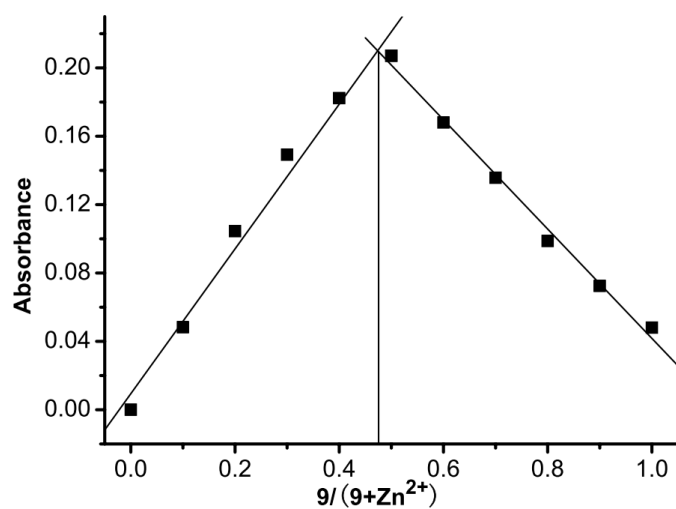


Figure. S31. Job's plot for determining the stoichiometry of **9** and  $Zn^{2+}$  in DMF.

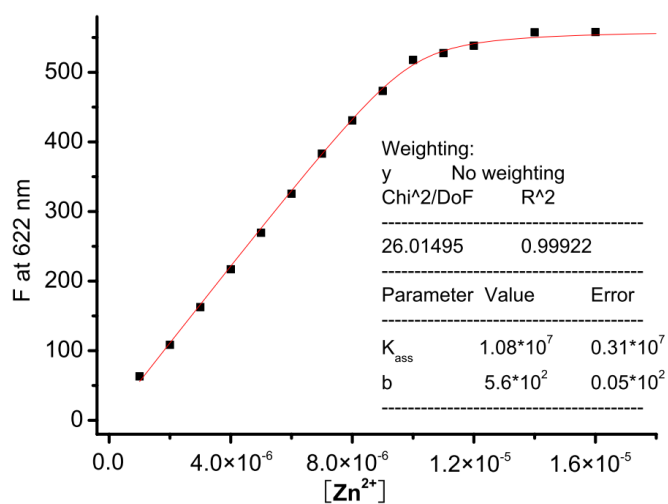


Figure. S32. Plot of  $F_{622nm}$  vs.  $[Zn^{2+}]$  for **9** in DMF.  $\lambda_{ex} = 538$  nm. The best fit line to the equation, superimposed on the data, yields  $K_{ass}$  of  $1.08 \times 10^7 M^{-1}$ .

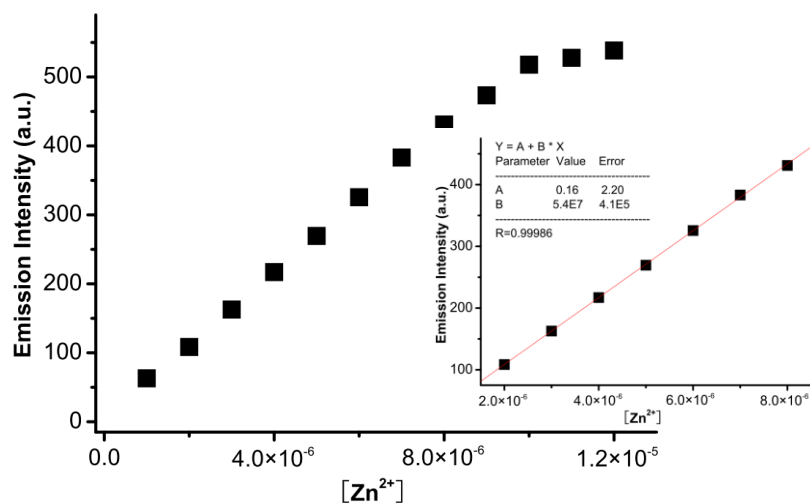


Figure. S33. Calibration curve of probe **9** in DMF, with the fluorescence intensity at 622 nm plotted vs  $Zn^{2+}$  concentration. The inset shows the linear responses at low  $Zn^{2+}$  concentrations.  $\lambda_{ex}$  was fixed at 538 nm. The detection limit was found to be  $1.1 \times 10^{-8}$  M.

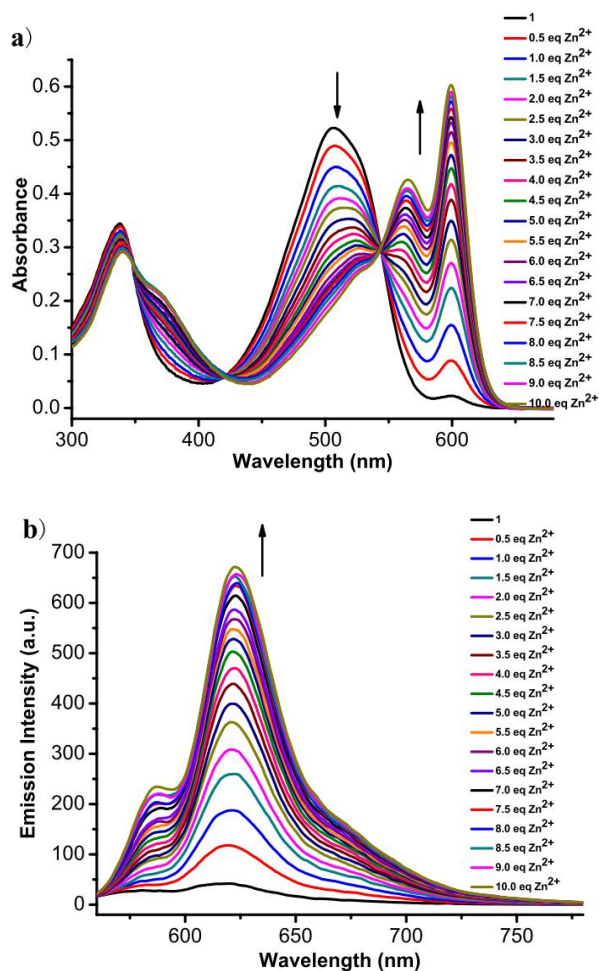


Figure. S34. a) Absorbance changes during the titration of **9** ( $10 \mu M$ ) with  $Zn^{2+}$  in the HEPES buffer (DMF/50mM HEPES, 4:1, v:v, pH 7.2). b) Fluorescence changes during the titration of **9** ( $10 \mu M$ ) with  $Zn^{2+}$  in the HEPES buffer. Excitation wavelength was fixed at 545 nm (one of the isosbestic points).